Disclaimer:

This manuscript is a non-peer-reviewed preprint submitted to EarthArXiv.

Chitosan-Modified Loofah Scaffold for Sustainable Microplastic Removal from Water

Sophia Zhao[1,2*], Preston Larson[3], Binbin Weng[1*]

[1]School of Electrical and Computer Engineering, University of Oklahoma, Norman, OK, USA
[2]Norman North High School, Norman, OK, USA
[3]Samuel Roberts Noble Microscopy Laboratory, University of Oklahoma, Norman, OK, USA
*Corresponding emails: sophia.w.zhao-1@ou.edu, binbinweng@ou.edu

Abstract: The global accumulation of over 400 million tons of plastic waste annually has intensified the growing crisis of micro- and nanoplastic (MNP) contamination in natural and drinking water systems. These particles persist in the environment and act as vectors for toxic pollutants. Existing mitigation strategies often rely on costly synthetic materials or energy-intensive infrastructure, which may generate secondary waste streams and limit accessibility in low-resource settings. Here, we develop a low-cost, biodegradable, easily fabricated filtration platform using chitosan-coated loofah scaffolds designed to remove microplastics across diverse size ranges and morphologies. Mechanically ground polystyrene (PS) particles spanning ~500 nm to several millimeters, including irregular fragments, fibers, and spheres, were used to model realistic morphological heterogeneity. Filtration performance was evaluated under both controlled laboratory conditions and in MNP-spiked environmental pond water to capture interference from naturally occurring organic matter. Removal efficiency was quantified using optical microscopy, while SEM and ATR-FTIR verified coating integrity and characterized interactions between PS particles and the chitosan-modified scaffold. The filters achieved a cumulative MNP removal efficiency exceeding 96%, with up to 98.4% removal across all size bins, and maintained stable performance over four filtration cycles. Importantly, high removal rates persisted in environmental water matrices, demonstrating robustness under realistic conditions. With a material cost of only $0.08 per unit and minimal fabrication requirements, chitosan-modified loofah filters offer a scalable and sustainable approach for microplastic mitigation, especially in regions lacking conventional water-treatment infrastructure, such as rural and developing areas.

Graphical Abstract:

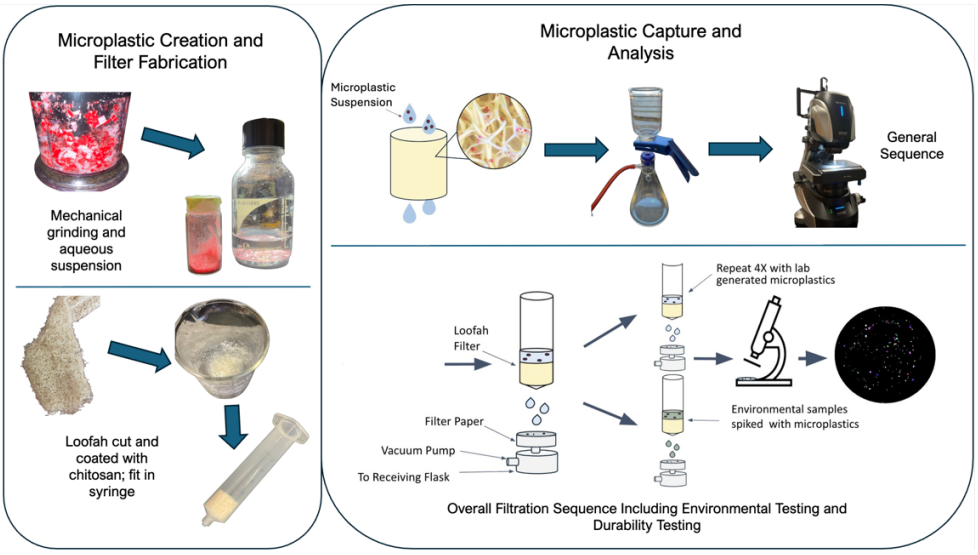

1. Introduction

Microplastics (MPs, <5 mm) and nanoplastics (NPs, <1 μm) (Hartmann et al., 2019) have emerged as pervasive and persistent contaminants in aquatic environments. Their widespread occurrence has been documented in surface water, groundwater, wastewater, and even treated drinking water(Thompson, 2024; Hoang et al., 2025), reflecting their growing infiltration across global water systems. MPs originate from the fragmentation of larger plastics, synthetic textiles, packaging materials, personal care products, and industrial effluents (Sangkham et al., 2022). Their small size, chemical stability, and resistance to biodegradation enable long-term environmental persistence once introduced into the environment.

Beyond physical presence, microplastics act as vectors for toxic contaminants. Their high surface-area-to-volume ratio facilitates adsorption of heavy metals and hydrophobic organic pollutants, promoting their transport through aquatic ecosystems (Rafa et al., 2024). Recent reports of microplastics in human blood and placental tissue highlight the potential for translocation across biological barriers, raising concerns about trophic transfer and human exposure (Sangkham et al., 2022, Leslie et al., 2022; Ragusa et al., 2021). Laboratory studies further demonstrate that microplastic exposure can trigger oxidative stress, inflammation, and cytotoxic effects in mammalian cells and animal models (Li et al., 2022; Schirinzi et al., 2017). Although long-term health implications remain uncertain, growing evidence of biological interactions highlights urgent needs for strategies that reduce human and ecological exposure, particularly through improved water treatment approaches. As understanding of microplastic transport and risks expands, the need for scalable and effective removal technologies has become increasingly urgent.

Despite increasing recognition of microplastic contamination, effective removal from water systems remains a substantial challenge. MPs span a broad spectrum of sizes, shapes, densities, and surface chemistries, including fragments, fibers, films, and spheres, many of which fall below the capture limits of conventional filtration technologies. Established removal strategies, including membrane filtration, coagulation, flocculation, activated carbon adsorption, and advanced oxidation, can achieve high removal efficiencies, but these processes often reply on energy-intensive operation, high material costs, or synthetic, non-biodegradable media (Dayal et al., 2024). Such constraints hinder widespread implementation and limit accessibility, particularly in regions lacking advanced water-treatment infrastructure (Mulindwa et al., 2024).

These limitations have stimulated interest in sustainable, bio-based filtration materials that offer low-cost, low-energy alternatives suitable for decentralized or resource-limited applications. Chitosan, a biodegradable polysaccharide derived from chitin, exhibits strong adsorption capacity and interacts readily with negatively charged pollutants, including microplastics (Prasetyo et al., 2025; Risch & Adlhart, 2021). Its amine-rich structure supports electrostatic attraction, hydrogen bonding, and chelation (Thambiliyagodage et al., 2023), making chitosan a versatile platform for pollutant binding. Recent chitosan-based filtration systems, including nanofiber composites and chitosan-modified membranes, have demonstrated promising removal efficiencies. However, many reply on specialized fabrication process, chemical crosslinking, or controlled model

particles, reducing scalability and limiting applicability in realistic environmental settings (Risch & Adlhart, 2021).

Natural loofah fibers present a complementary bio-based scaffold with inherent porosity, high surface area, and mechanical stability. Modified loofah systems have achieved high removal efficiencies for synthetic fibers and microplastic particles. Rathinamoorthy et al., 2025 demonstrated that alkali-treated loofah fibers, structured into densely packed filtration columns, effectively removed polyester microfibers from simulated laundry effluent, achieving average removal efficiencies of 94-98% under optimized packing conditions. This performance was attributed primarily to reduced pore size and increased surface roughness following alkali treatment, which enhanced mechanical retention of fibers. Similarly, Ha et al., 2023 developed superhydrophobic loofah sponges via wax-based surface modification and reported high microplastic removal efficiencies up to 99% for 5 μm polystyrene microspheres. Despite these advances, existing studies typically employ monodisperse or simplified microplastic models. Critical gaps remain regarding size-dependent capture performance, removal of smaller microplastic fractions, and filtration behavior under environmentally complex conditions such as high organic content or competing natural particulates.

To address these gaps, this study develops a chitosan-coated loofah filtration system that integrates a naturally abundant fibrous scaffold with a functional biopolymer layer to capture microplastics efficiently and sustainably. Mechanically generated polystyrene particles spanning multiple size bins and morphologies were used to represent realistic physical heterogeneity, while testing in microplastic-spiked pond water enabled evaluation environmentally relevant matrix conditions. By combining sustainable materials with realistic particle models and complex water matrices, this work provides a mechanistically grounded and application-oriented assessment of bio-based microplastic filtration. These findings support the development of scalable, low-cost solutions for microplastic removal in settings where conventional water treatment technologies remain inaccessible.

2. Materials and Methods

2.1 Microplastic Preparation

Red colored polystyrene drinking cups (Great Value Party Plastic Cups 18oz) were mechanically ground to produce irregular fragments that mimic environmentally weathered microplastics in shape and size heterogeneity. The resulting particles were suspended in distilled water at a controlled concentration of 10 mg/L. Particle size distribution was characterized using area-based bins ranging from <150 μm² to >50,000 μm² to capture a broad spectrum of fragment sizes.

To promote uniform particle dispersion prior to filtration, suspensions were manually homogenized immediately before each trial. Each solution was gently swirled in a circular motion for 10 -15 seconds, followed by 30 full inversions (180° rotations) at approximately one inversion per second. The suspension was then allowed to rest for 5 seconds to reduce turbulence while maintaining homogeneous particle distribution before filtration.

For environmental condition testing, pond water was collected locally and passed through a coarse mesh to remove large debris and suspended macro-particulates. The filtered environmental water was subsequently spiked with microplastics to the same target concentration (10 mg/L) to simulate realistic organic and particulate interference conditions during filtration testing.

2.2 Loofah Scaffold Fabrication

Natural loofah sponges were rinsed multiple times with distilled water to remove residual impurities and particulates, then air-dried for 24 hours. The dried material was cut into cylindrical scaffolds measuring 2 × 2 cm.

Chitosan powder (Sigma-Aldrich, CAS: 9012-76-4) was dissolved in 1% (v/v) acetic acid under continuous magnetic stirring to prepare a 1.5% (w/v) solution. The loofah scaffolds were immersed in the chitosan solution to allow uniform coating and infiltration throughout the porous matrix, forming chitosan-modified biofilters. Coated scaffolds were air-dried for 12 hours to permit solvent evaporation and stabilization of the chitosan layer.

Each scaffold was then placed into a syringe-based flow-through filtration apparatus for subsequent performance testing.

2.3 Filtration Testing

A vertical syringe system was used to maintain controlled gravity-driven flow. The plunger was removed and the microplastic solution was introduced into the barrel containing the loofah scaffold. Each trial consisted of 250 mL of microplastic solution (10 mg/L) per cycle and three independent loofahs replicated per condition (n=3).

Testing conditions included: unfiltered microplastic solution (MP-Ctrl), uncoated loofah filter (LF), chitosan-coated loofah filter (CLF), and environmental water-tested coated loofah filter (CLF-Env).

A blank control of distilled water filtered through CLF was used to assess contamination contribution from the surroundings.

2.4 Optical Microscopy and Quantification

Effluent samples collected following filtration were vacuum filtered through glass microfiber filter paper (pore size 1.2 μm) to capture residual microplastic particles. The entire filtered volume was processed for each sample to ensure accurate concentration measurements. Filters were dried at room temperature in a covered environment to prevent airborne contamination prior to imaging.

Captured microplastics were imaged using optical microscopy under standardized magnification, illumination intensity, exposure time, and gain settings. Imaging parameters were fixed across all experimental groups (MP-Ctrl, LF, CLF, and CLF-Env)

to ensure consistency. Multiple non-overlapping fields of view were acquired per filter and stitched to represent the full filter surface area.

Image analysis was performed using color threshold segmentation. A fixed red-channel intensity range was defined using baseline microplastic control images and applied uniformly across all samples to eliminate operator bias. Segmented particles were automatically quantified to obtain:

- Total particle count
- Projected particle area (μm²), calculated from calibrated pixel size
- Equivalent diameter and size distribution

Pixel-to-length calibration was performed using the microscope scale bar. Projected area values were derived by converting pixel area to physical units using:

$$\text{Area} = \text{pixel count} \times (\text{pixel size})^2$$

Particles were grouped into predefined size bins to assess size-dependent filtration performance.

Particle concentration (particles/mL) was calculated by normalizing total particle counts to the volume of effluent filtered. Baseline concentration (C_{in}) was determined from the unfiltered microplastic control (MP-Ctrl), while post-filtration concentration (C_{out}) was determined from effluent samples.

Removal efficiency was calculated as:

$$\text{Removal Efficiency (\%)} = \frac{C_{in} - C_{out}}{C_{in}} \times 100$$

where:

- C_{in}= baseline particle/area concentration (particles/mL)
- C_{out}= particle/area concentration after filtration

Particle count removal alone does not fully capture filtration performance because microplastics vary dramatically in size and morphology. A system could remove many small particles while allowing fewer but larger fragments to pass through, resulting in a high particle-count efficiency but lower mass or surface-area removal. To address this, projected particle area removal (%) was calculated complementary to particle count removal using total projected particle area per milliliter to evaluate the removal of microplastic mass proxies.

2.5 Structural and Chemical Characterization

Attenuated Total Reflectance Fourier Transform Infrared (ATR-FTIR) spectroscopy (*Bruker Invenio-R*), was performed to confirm successful chemical functionalization of the

loofah scaffold following chitosan coating. Spectra were acquired to identify characteristic cellulose bands and the emergence of chitosan-specific functional groups, including amide I and amide II vibrations, thereby verifying surface modification.

Scanning Electron Microscopy (SEM) using a Thermoscientific Quattro S environmental SEM in low vacuum mode was used to characterize the surface morphology and pore architecture of both uncoated loofah (LF) and chitosan-coated loofah (CLF) scaffolds. High-resolution imaging enabled comparison of pore size distribution and chitosan deposition within the porous matrix. Post-filtration SEM analysis further confirmed the retention of MNPs within chitosan-filled pores and along coated fiber surfaces, providing direct morphological evidence of particle capture.

2.6 Reusability Assessment

To evaluate filter durability and reusability, each chitosan-coated loofah (CLF) scaffold was subjected to four consecutive 250 mL filtration cycles under identical experimental conditions. Removal efficiency was measured after each cycle to assess performance stability over repeated use.

2.7 Statistical Analysis

The following statistical analyses were performed to evaluate filtration performance, reusability, and size-selective effects. One-way analysis of variance (ANOVA) was used to compare mean removal efficiencies across experimental groups. When a significant overall group effect was detected, post hoc pairwise comparisons (Tukey's Honestly Significant Difference test) were conducted to determine which specific groups differed from one another while controlling for Type I error.

To assess performance stability across sequential filtration cycles, linear analysis was performed with removal efficiency modeled as a function of filtration cycle number. This approach allowed evaluation of directional trends (e.g., performance decline or conditioning effects) over repeated use.

Differences in microplastic size distribution among filtration conditions were assessed using a chi-square test of homogeneity. When significant distributional differences were observed, standardized residual analysis was conducted to identify which size bins contributed most strongly to the chi-square statistic.

Statistical significance was defined at a threshold of $\alpha = 0.05$.

3. Results and Discussion

3.1 ATR-FTIR Confirmation of Chitosan Functionalization

ATR-FTIR analysis confirmed successful surface modification of the cellulose-based loofah scaffold with chitosan (Figure 1). Raw loofah displayed characteristic cellulose peaks, including broad O–H stretching (~3300–3400 cm^{-1}), C–H stretching (~2900 cm^{-1}),

and C–O–C/C–O vibrations between 1000–1160 cm^{-1} (Kasaai, 2008; Oh et al., 2005). After coating, new absorption bands appeared that are characteristic of chitosan, including the amide I (~1645 cm^{-1}) and amide II (~1550 cm^{-1}) bands, along with an intensified O–H/N–H region (~3200–3500 cm^{-1}). These spectral changes confirm the presence of chitosan in the cellulose-based loofah scaffold (Kasaai, 2008).

The overlap between the spectra of cellulose and chitosan in the hydroxyl region suggests hydrogen bonding interactions between the two materials, indicating strong interfacial adhesion rather than simple physical adsorption (Rinaudo, 2006).

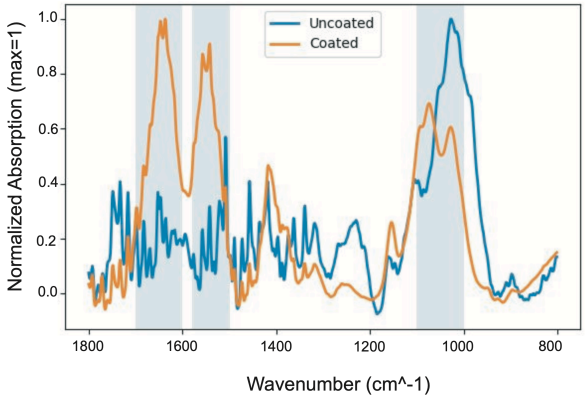

Figure 1: ATR-FTIR confirmation of chitosan coating on loofah fibers.
ATR-FTIR spectra (800–1800 cm−1) of uncoated and chitosan-coated loofah after baseline correction using asymmetric least squares (ALS) and peak-height normalization (max = 1). Shaded regions indicate characteristic vibrational bands: amide I (1600–1700 cm−1), amide II (1500–1580 cm−1), and cellulose C–O–C/C–O stretching (1000–1100 cm−1).

The incorporation of protonatable amine groups (-NH_2), provides sites for electrostatic interactions with negatively charged microplastics (Dash et al., 2011), forming the chemical basis for enhanced capture efficiency described below.

3.2 Removal Efficiency and Influence of Chitosan Functionalization

a) First-pass performance

After three replicates, the chitosan-coated loofah filter (CLF) exhibited significantly higher microplastics removal efficiency than the uncoated loofah (LF). Mean particle removal efficiency for CLF was 93.2% ± 0.7 (SE), compared to 68.4% ± 2.1 (SE) for LF (Figure 2A-2D). Area-based removal showed a similar trend: CLF achieved 92.9%% ±1.3 (SE), while LF achieved 73.6% ± 5.8 (SE). When tested with microplastic-spiked environmental pond water, CLF-Env maintained comparable efficiency at 92.6% ± 2.6 (SE).

One-way ANOVA confirmed significant differences across LF, CLF, and CLF-Env ($p < 0.001$). Post hoc Tukey analysis indicated that CLF significantly outperformed LF ($p < 0.001$), while CLF and CLF-Env were statistically indistinguishable ($p > 0.05$), demonstrating robustness in environmental matrices. Compared to the uncoated loofah, the chitosan-modified scaffold showed a statistically significant improvement in removal efficiency, confirming that chemical surface modification rather than mechanical structure alone is primarily responsible for the enhanced capture behavior.

Environmental matrices typically contain dissolved organic matter and suspended particulates that can interfere with adsorption-based systems (Ling et al., 2020). As performance in microplastic-spiked environmental pond water remained comparable to distilled-water trials, with no statistically significant difference in removal efficiency, the retention of high efficiency under these conditions suggests that the dominant capture

mechanisms are sufficiently robust to withstand moderate environmental interference, supporting potential application in real-life water systems.

b) Repeated-cycle stability

To evaluate performance stability across repeated use, particle removal efficiencies from four sequential filtration cycles were analyzed using both one-way ANOVA and linear regression (Figure 2E). One-way ANOVA revealed no statistically significant overall difference in removal efficiency among the four cycles ($p = 0.11$), indicating that filtration performance did not significantly change with repeated use. Because filtration cycles represent an ordered sequence, linear regression was additionally performed to assess the presence of a directional trend. Regression analysis demonstrated a positive slope of approximately 1.3% increase in removal efficiency per cycle ($R^2 = 0.82$), suggesting a potential upward trend consistent with early-stage filter conditioning. However, this trend did not reach statistical significance ($p = 0.095$). Total particle removal efficiency over the 1 L was calculated to be 96% ± 1.3 (SE). Area-based removal efficiency showed a similar pattern to particle-count removal across sequential cycles. Together, these analyses indicate that the chitosan-coated loofah maintained statistically stable performance across sequential filtrations, with a non-significant trend toward improved efficiency rather than decline.

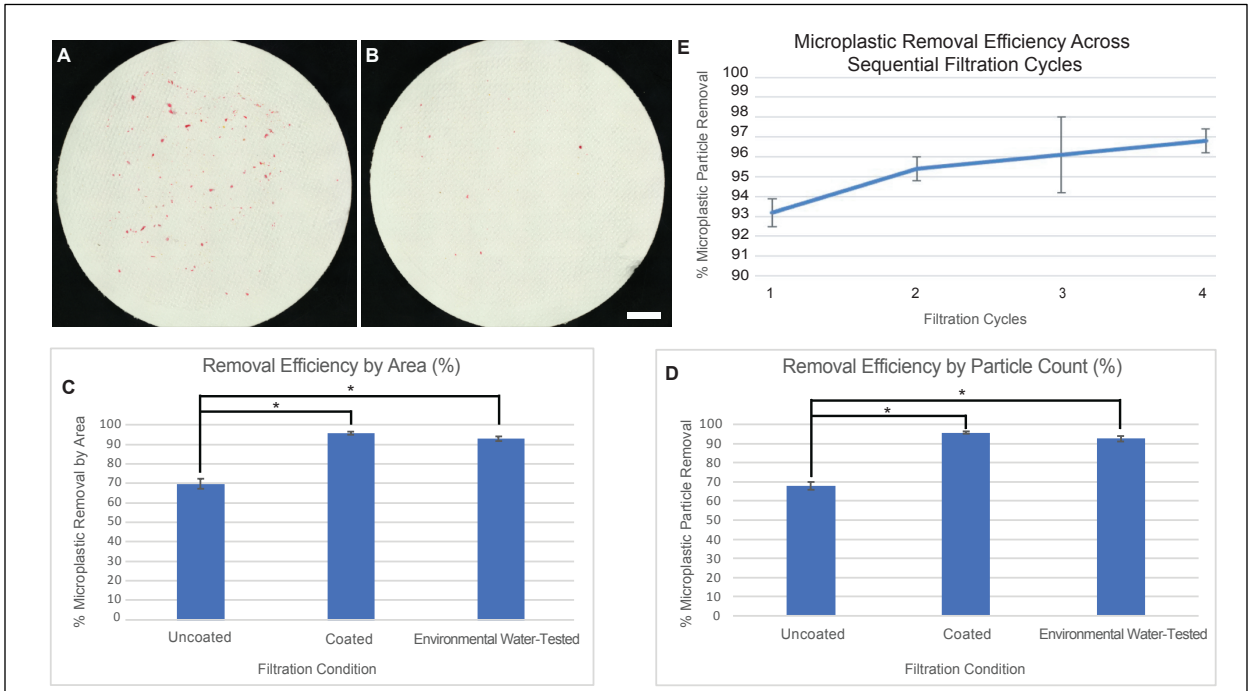

Figure 2. Removal efficiency of microplastics by the chitosan-coated loofah filtration system.
(A,B) Optical microscopy of microplastics retained on a glass filter after filtration through an uncoated loofah (LF) (A) and a chitosan-coated loofah (CLF) (B), showing reduced retention of smaller particles after chitosan coating. Removal efficiency by particle count (C) and area (D) for LF, CLF, and environmental water - tested chitosan-coated loofah (CLF-Env) filters. (E) Removal efficiency across sequential filtration cycles shows sustained performance. Data are mean ± SD (n = 3); asterisks indicate significant differences (one-way ANOVA with Tukey's post hoc test, *$p < 0.001$). Scale bars = 5000 µm.

The absence of performance degradation indicates strong interfacial adhesion between chitosan and cellulose fibers and suggests that the coating remains structurally stable

under repeated hydraulic exposure. The observed trend of slight efficiency increase across cycles may reflect early-stage conditioning of the chitosan-coated scaffold, where initial particle deposition modifies the effective pore structure and enhances subsequent capture, consistent with findings that particle deposition alters effective filtration area and impacts capture behavior in porous filter media (Guo et al., 2025). This stability supports the feasibility of multi-use operation prior to regeneration or replacement, an important consideration for practical deployment.

3.3 Size-Selective Capture

As shown in Figure 3, Microplastics collected from effluent samples were categorized into fixed size bins (0-150 µm, 150-1000 µm, 1000-50,000 µm, and >50,000 µm) to evaluate size-selective filtration behavior. A chi-square test of homogeneity comparing size distributions before and after filtration revealed a statistically significant redistribution of particle sizes ($p < 0.001$), indicating that removal was not uniform across bins. Standardized residual analysis further identified the 0-150 µm bin as the primary contributor to the chi-square statistic, demonstrating disproportionately high removal of smaller particles relative to expectation. Moderate reductions were also observed across larger size bins, though these contributed less strongly to the overall distributional shift.

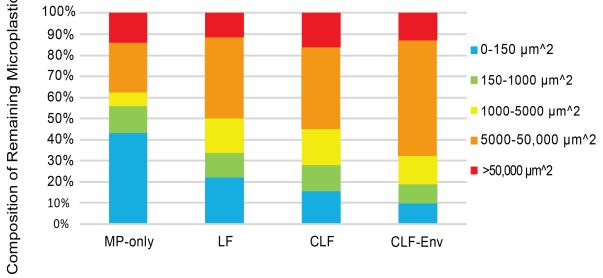

Figure 3. Size-selective microplastic removal by chitosan-coated loofah filtration.
Size distribution of remaining microplastics after filtration under four conditions, Microplastics without being filtered (MP-only), LF, CLF, and CLF-Env. Bars represent mean normalized composition (n = 3). Chitosan coating significantly reduces small microplastic fractions (0-150 and 150-1000 µm).

This behavior suggests that surface-dominated interactions play an increasingly important role as particle size decreases. Smaller particles possess higher surface area-to-volume ratios and greater diffusion-driven mobility, increasing their likelihood of contact with reactive fiber surfaces (E. Essien et al., 2025; Douverne & Hoffmann, 2025). Because projected area disproportionately reflects larger fragments, CLF's area removal values were slightly lower than particle-count removal. This difference supports the claim of preferential capture of smaller particles by the chitosan-coated scaffold, while larger fragments contribute more heavily to residual total area despite lower numerical abundance. The selective reduction of smaller size fractions is particularly significant because these particles pose elevated ecological and biological risks and are often more difficult to remove using conventional filtration materials (Bucci & Rochman, 2022; E. Essien et al., 2025).

3.4 SEM Confirmation of Chitosan-Affected Morphology and Nanoplastics Removal

SEM imaging from Figure 4 demonstrated that chitosan functionalization reduced the effective pore diameter and increased surface roughness relative to the uncoated loofah scaffold (Figure 4A). The chitosan coating formed a conformal layer along fiber surfaces and partially filled larger pore openings, resulting in a denser and more heterogeneous microstructure (Figure 4B).

Post-filtration SEM analysis revealed clear microplastic adhesion within coated pore structures (Figure 3C) and along chitosan-coated fiber surfaces (Figure 3D). In addition to micron-scale fragments, nanoplastic-scale particles were observed embedded within the chitosan matrix in Figure 3C and 3D, providing direct morphological evidence of surface-mediated capture mechanisms. These observations support the role of chitosan in enhancing particle retention through increased surface interaction and reduced pore accessibility.

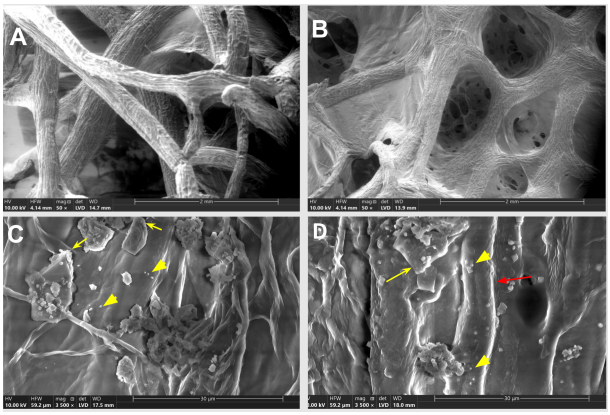

Figure 4: SEM comparison of loofah pore sizes and confirmation of nanoplastic capture.
SEM images show the porous structure of uncoated loofah (A) and reduced pore size after chitosan coating (B) while maintaining an interconnected fibrous scaffold. Higher-magnification images reveal micro- and nanoplastics adhered to chitosan-modified pore regions (C) and loofah fiber surfaces (D). Yellow arrowheads indicate nanoparticles, yellow arrows indicate microparticles, and red arrows highlight loofah fiber structure. Scale bar: 2mm (A and B) and 30 μm (C and D).

3.5 Contamination Assessment

Blank control filtration of distilled water resulted in minimal background contamination (~0.07 particles/mL), substantially lower than experimental concentrations. This confirms that observed removal efficiencies reflect true filtration performance rather than environment-derived artifacts.

3.6 Mechanistic Interpretation of Capture Behavior

The improved performance arises from the synergistic interaction between the loofah's hierarchical porous architecture and the reactive surface chemistry of chitosan. The native loofah provides a three-dimensional, interconnected cellulose network that enables mechanical interception of larger particles while maintaining high permeability. Upon coating, chitosan introduces protonatable amine groups and increases fiber surface roughness, partially reducing effective pore diameter. These changes enhance both electrostatic attraction and surface-mediated adhesion between the scaffold and microplastic particles. Under neutral to mildly acidic conditions, the amine groups can become partially protonated, promoting electrostatic interactions with negatively charged microplastic surfaces (da Silva Alves et al., 2021). In addition, hydrogen bonding and van der Waals interactions contribute to particle retention within the modified pore network (Yang et al., 2025).

3.7 Comparison with Conventional Microplastic Mitigation Technologies

Compared to conventional microplastic mitigation technologies, such as membrane filtration or synthetic polymer adsorbents, the chitosan-loofah scaffold offers substantial sustainability advantages. The materials are biodegradable, low-cost (approximately $0.08 per unit), and require no advanced manufacturing infrastructure. While certain high-end membrane systems may achieve similar removal percentages, they often depend on energy input and non-biodegradable materials (Ezugbe & Rathilal, 2020). In contrast, this cost-effective natural system demonstrates the competitive performance while aligning

with green chemistry and circular material principles.

4. Conclusion and Future Prospects

This study demonstrates that a chitosan-modified loofah scaffold can function as a highly efficient, biodegradable, and mechanically robust biofilter for microplastic removal from water. The coated system achieved >96% average cumulative removal frequency and >93% first-pass average removal efficiency across diverse particle morphologies and size ranges, including sub-micron particles, while maintaining stable performance over four sequential filtration cycles. Importantly, high removal efficiency was preserved in environmentally spiked pond water, indicating resilience in complex natural matrices. Mechanistically, enhanced performance arises from the synergistic integration of loofah's hierarchical porous architecture with chitosan's reactive amine-rich surface chemistry. The loofah scaffold provides macroscopic permeability and mechanical entrapment, while chitosan introduces protonatable amine groups that promote electrostatic attraction, hydrogen bonding, and surface adhesion. Preferential removal of smaller particles suggests that surface-mediated interactions dominate capture at lower size scales, where diffusion and surface area effects increase contact probability. Compared to conventional synthetic filtration materials, this platform offers significant advantages in sustainability, cost (~$0.08 per unit), biodegradability, and fabrication simplicity. The ability to maintain high efficiency without performance decay supports its potential for repeated use in decentralized water treatment applications. Collectively, these findings establish chitosan-modified loofah as a scalable, environmentally responsible engineering solution that bridges material science, green chemistry, and water treatment technology.

While the filtration system demonstrated high efficiency and stability under the tested conditions, some limitations remain that warrant further investigation in future. Long-term durability beyond four sequential filtration cycles was not assessed, and future work should determine the maximum number of operational cycles prior to performance declining below 86% (defined as a 10% reduction from the initial average efficiency). Establishing this threshold will provide a practical engineering benchmark for filter lifespan and regeneration scheduling. Additionally, while microplastic-spiked environmental water was evaluated, further testing is needed using water samples containing naturally occurring microplastics from diverse sources such as wastewater effluent, storm runoff, and both flowing and standing freshwater systems. These studies would better represent real-world particle heterogeneity and environmental complexity. Beyond capture efficiency, post-capture management of retained microplastics remains an important consideration. Future designs may integrate enzymatic or catalytic components, such as plastic-degrading enzymes or photocatalytic materials, to promote partial degradation of captured particles and reduce long-term waste accumulation (Cavalcante et al., 2025; Guan et al., 2025; Gupta et al., 2025). Finally, the multifunctional properties of chitosan merit deeper exploration. Its inherent antimicrobial activity, metal-ion binding capacity, and tunable surface chemistry may further enhance filter longevity, broaden contaminant removal capabilities, and improve overall system performance beyond microplastic

capture alone (Saheed et al., 2021; Elzahar & Bassyouni, 2023; Ngah et al., 2005; Rinaudo, 2006). Together, these future directions would advance the scaffold from a proof-of-concept biofilter to a scalable, multifunctional water treatment platform.

References

Bucci, K., & Rochman, C. M. (2022). Microplastics: A multidimensional contaminant requires a multidimensional framework for assessing risk. *Microplastics and Nanoplastics*, *2*(1), 7. https://doi.org/10.1186/s43591-022-00028-0

Cavalcante, A. L. G., Dari, D. N., de Morais Silva, M. F., da Silva Vieira, R., da Silva Aires, F. I., de Sousa, P. G., dos Santos, K. M., & dos Santos, J. C. S. (2025). Advances in enzymatic degradation of microplastics: Mechanisms, optimization strategies, and future directions. *Molecular Catalysis*, *585*, 115392. https://doi.org/10.1016/j.mcat.2025.115392

da Silva Alves, D. C., Healy, B., Pinto, L. A. de A., Cadaval, T. R. S., & Breslin, C. B. (2021). Recent Developments in Chitosan-Based Adsorbents for the Removal of Pollutants from Aqueous Environments. *Molecules*, *26*(3), 594. https://doi.org/10.3390/molecules26030594

Dash, M., Chiellini, F., Ottenbrite, R. M., & Chiellini, E. (2011). Chitosan—A versatile semi-synthetic polymer in biomedical applications. *Progress in Polymer Science, Special Issue on Biomaterials*, *36*(8), 981–1014. https://doi.org/10.1016/j.progpolymsci.2011.02.001

Dayal, L., Yadav, K., Dey, U., Das, K., Kumari, P., Raj, D., & Mandal, R. R. (2024). Recent advancement in microplastic removal process from wastewater—A critical review. *Journal of Hazardous Materials Advances*, *16*, 100460. https://doi.org/10.1016/j.hazadv.2024.100460

Douverne, M., & Hoffmann, T. (2025). When Size Matters: Size-Selective Chemistry in the Heterogeneous Processing of Organic Aerosols. *ACS ES&T Air*, *2*(11), 2491–2503. https://doi.org/10.1021/acsestair.5c00189

E. Essien, A., E. Dickson-Anderson, S., & Guo, Y. (2025). *Microplastics and nanoplastics in stormwater management engineered porous media systems: A systematic review of their sources, transport, retention, and removal characteristics*. https://doi.org/10.1039/D5VA00169B

Elzahar, M. M. H., & Bassyouni, M. (2023). Removal of direct dyes from wastewater using chitosan and polyacrylamide blends. *Scientific Reports*, *13*(1), 15750. https://doi.org/10.1038/s41598-023-42960-y

Ezugbe, E. O., & Rathilal, S. (2020). Membrane Technologies in Wastewater Treatment: A Review. *Membranes*, *10*(5). https://doi.org/10.3390/membranes10050089

Guan, G., Ren, W., Huo, S., Zou, B., Qian, J., Wang, F., Ma, A., Zhuang, G., & Xu, L. (2025). Photocatalytic and Enzymatic Degradation of Microplastics: Current Status, Comparison, and Combination. *Catalysts*, *15*(11). https://doi.org/10.3390/catal15111015

Guo, C., Kang, J., Wang, D., Liang, Y., Wang, L., Xu, G., Wang, H., & Tang, M. (2025). Experimental and Simulation Study of Particle Deposition Characteristics and Pressure Drop Evolution in Pleated Filter Media. *Processes*, *13*(4), 975. https://doi.org/10.3390/pr13040975

Gupta, G. K., Dixit, M., Chot, E., & Shukla, P. (2025). Insights into Microbial Enzymatic Biodegradation of Plastics and Microplastics: Technological Updates. *ACS Environmental Au*, *5*(6), 520–542. https://doi.org/10.1021/acsenvironau.5c00033

Ha, T. T. V., Viet, N. M., Thanh, P. T., & Quan, V. T. (2023). Loofah plant—Derived biodegradable superhydrophobic sponge for effective removal of oil and

microplastic from water. *Environmental Technology & Innovation*, *32*, 103265. https://doi.org/10.1016/j.eti.2023.103265

Hartmann, N. B., Hüffer, T., Thompson, R. C., Hassellöv, M., Verschoor, A., Daugaard, A. E., Rist, S., Karlsson, T., Brennholt, N., Cole, M., Herrling, M. P., Hess, M. C., Ivleva, N. P., Lusher, A. L., & Wagner, M. (2019). Are We Speaking the Same Language? Recommendations for a Definition and Categorization Framework for Plastic Debris. *Environmental Science & Technology*, *53*(3), 1039–1047. https://doi.org/10.1021/acs.est.8b05297

Hoang, V.-H., Nguyen, M.-K., Hoang, T.-D., Rangel-Buitrago, N., Lin, C., Pham, M.-T., Ha, M. C., Nguyen, T. P., Shaaban, M., Chang, S. W., & Nguyen, D. D. (2025). Microplastic characteristics, transport, risks, and remediation in groundwater: A review. *Environmental Chemistry Letters*. https://doi.org/10.1007/s10311-025-01825-8

Kasaai, M. R. (2008). A review of several reported procedures to determine the degree of *N*-acetylation for chitin and chitosan using infrared spectroscopy. *Carbohydrate Polymers*, *71*(4), 497–508. https://doi.org/10.1016/j.carbpol.2007.07.009

Leslie, H. A., van Velzen, M. J. M., Brandsma, S. H., Vethaak, A. D., Garcia-Vallejo, J. J., & Lamoree, M. H. (2022). Discovery and quantification of plastic particle pollution in human blood. *Environment International*, *163*, 107199. https://doi.org/10.1016/j.envint.2022.107199

Li, X., Zhang, T., Lv, W., Wang, H., Chen, H., Xu, Q., Cai, H., & Dai, J. (2022). Intratracheal administration of polystyrene microplastics induces pulmonary fibrosis by activating oxidative stress and Wnt/β-catenin signaling pathway in

mice. *Ecotoxicology and Environmental Safety*, *232*, 113238. https://doi.org/10.1016/j.ecoenv.2022.113238

Ling, Y., Alzate-Sánchez, D. M., Klemes, M. J., Dichtel, W. R., & Helbling, D. E. (2020). Evaluating the effects of water matrix constituents on micropollutant removal by activated carbon and β-cyclodextrin polymer adsorbents. *Water Research*, *173*, 115551. https://doi.org/10.1016/j.watres.2020.115551

Mulindwa, P., Kasule, J. S., Nantaba, F., Wasswa, J., & Expósito, A. J. (2024). Bioadsorbents for removal of microplastics from water ecosystems: A review. *International Journal of Sustainable Engineering*, *17*(1), 582–599. https://doi.org/10.1080/19397038.2024.2374003

Ngah, W. S. W., Ab Ghani, S., & Kamari, A. (2005). Adsorption behaviour of Fe(II) and Fe(III) ions in aqueous solution on chitosan and cross-linked chitosan beads. *Bioresource Technology*, *96*(4), 443–450. https://doi.org/10.1016/j.biortech.2004.05.022

Oh, S. Y., Yoo, D. I., Shin, Y., & Seo, G. (2005). FTIR analysis of cellulose treated with sodium hydroxide and carbon dioxide. *Carbohydrate Research*, *340*(3), 417–428. https://doi.org/10.1016/j.carres.2004.11.027

Prasetyo, S., Santos, C. A., Sugih, A. K., & Kristianto, H. (2025). Utilization of chitosan as a natural coagulant for polyethylene microplastic removal. *Sustainable Chemistry for the Environment*, *9*, 100225. https://doi.org/10.1016/j.scenv.2025.100225

Rafa, N., Ahmed, B., Zohora, F., Bakya, J., Ahmed, S., Ahmed, S. F., Mofijur, M., Chowdhury, A. A., & Almomani, F. (2024). Microplastics as carriers of toxic

pollutants: Source, transport, and toxicological effects. *Environmental Pollution*, *343*, 123190. https://doi.org/10.1016/j.envpol.2023.123190

Ragusa, A., Svelato, A., Santacroce, C., Catalano, P., Notarstefano, V., Carnevali, O., Papa, F., Rongioletti, M. C. A., Baiocco, F., Draghi, S., D'Amore, E., Rinaldo, D., Matta, M., & Giorgini, E. (2021). Plasticenta: First evidence of microplastics in human placenta. *Environment International*, *146*, 106274. https://doi.org/10.1016/j.envint.2020.106274

Rathinamoorthy, R., Logitha, N., Jordan, J., Shriniha, P. K., & Sujitha, R. (2025). Mitigation of microfibers in laundry effluent: Investigation of luffa fibers as an eco-friendly filtration system. *Journal of Environmental Management*, *375*, 124251. https://doi.org/10.1016/j.jenvman.2025.124251

Rinaudo, M. (2006). Chitin and chitosan: Properties and applications. *Progress in Polymer Science*, *31*(7), 603–632. https://doi.org/10.1016/j.progpolymsci.2006.06.001

Risch, P., & Adlhart, C. (2021). A Chitosan Nanofiber Sponge for Oyster-Inspired Filtration of Microplastics. *ACS Applied Polymer Materials*, *3*(9), 4685–4694. https://doi.org/10.1021/acsapm.1c00799

Saheed, I. O., Oh, W. D., & Suah, F. B. M. (2021). Chitosan modifications for adsorption of pollutants – A review. *Journal of Hazardous Materials*, *408*, 124889. https://doi.org/10.1016/j.jhazmat.2020.124889

Sangkham, S., Faikhaw, O., Munkong, N., Sakunkoo, P., Arunlertaree, C., Chavali, M., Mousazadeh, M., & Tiwari, A. (2022). A review on microplastics and nanoplastics in the environment: Their occurrence, exposure routes, toxic studies, and

potential effects on human health. *Marine Pollution Bulletin*, *181*, 113832. https://doi.org/10.1016/j.marpolbul.2022.113832

Schirinzi, G. F., Pérez-Pomeda, I., Sanchís, J., Rossini, C., Farré, M., & Barceló, D. (2017). Cytotoxic effects of commonly used nanomaterials and microplastics on cerebral and epithelial human cells. *Environmental Research*, *159*, 579–587. https://doi.org/10.1016/j.envres.2017.08.043

Thambiliyagodage, C., Jayanetti, M., Mendis, A., Ekanayake, G., Liyanaarachchi, H., & Vigneswaran, S. (2023). Recent Advances in Chitosan-Based Applications—A Review. *Materials*, *16*(5), 2073. https://doi.org/10.3390/ma16052073

Thompson, R. C. (2024). *Twenty years of microplastic pollution research—What have we learned?* https://www.science.org/doi/10.1126/science.adl2746

Yang, Y., Yan, W., Ma, J., Carmona, D., Zhou, C., Nguyen, E., & Qiu, J. (2025). Fish Gill-Inspired Bidirectional Porous Polysaccharide Aerogels for Micro/Nanoplastics Removal. *ACS Applied Materials & Interfaces*, *17*(46), 63488–63499. https://doi.org/10.1021/acsami.5c18203